

Cosmological Constraints on Late-time Entropy Production

M. Kawasaki and K. Kohri

Research Center for the Early Universe, Faculty of Science, The University of Tokyo, Tokyo 113-0033, Japan

Naoshi Sugiyama

Department of Physics, Kyoto University, Kyoto 606-8502, Japan

We investigate cosmological effects concerning the late-time entropy production due to the decay of non-relativistic massive particles. The thermalization process of neutrinos after the entropy production is properly solved by using the Boltzmann equation. If a large entropy production takes place at late time $t \simeq 1$ sec, it is found that a large fraction of neutrinos cannot be thermalized. This fact loosens the tight constraint on the reheating temperature T_R from the big bang nucleosynthesis and T_R could be as low as 0.5 MeV. The influence on the large scale structure formation and cosmic microwave background anisotropies is also discussed.

98.80.Cq, 98.70.Vc

RESCEU 7/99, KUNS-1546, astro-ph/9811437

It is usually believed that thermal radiation dominates the energy density of the early universe after the reheating process of the primordial inflation. At least, the universe is expected to be radiation-dominated before the big bang nucleosynthesis (BBN) epoch ($t \simeq 1$ sec) otherwise the abundances of the synthesized light elements (^4He , ^3He , D and ^7Li) do not agree with observations [1]. However, it is uncertain that the universe is radiation dominated before BBN epoch. In fact, particle physics models beyond the standard one predict a number of new massive particles some of which have long lifetimes and may influence the standard BBN scenario. Since the energy density of such massive non-relativistic particles decreases more slowly than that of the radiation as the universe expands, the universe becomes matter-dominated by those particles until they decay. When they decay into ordinary particles, the large entropy is produced and universe becomes radiation-dominated again. We call this process “late-time entropy production”.

One can find some interesting candidates for the late-time entropy production in models based on supersymmetry (SUSY). In local SUSY (i.e. supergravity) theories [2] there exist gravitino and Polonyi field [3] which have masses of $\sim \mathcal{O}(100\text{GeV} - 10\text{TeV})$. Since gravitino and Polonyi field interact with other particles only through gravity, they have long lifetimes. For example, the Polonyi field with mass ~ 10 TeV quickly dominates the energy density of the universe because this field cannot be diluted by usual inflation and decays at BBN epoch. It is also known that superstring theories have many light fields such as dilaton and moduli which have similar properties as the Polonyi field.

When one considers the late-time entropy production, reheating temperature T_R is usually used as a parameter to characterize it. The reheating temperature T_R is determined from $\Gamma = 3H(T_R)$ where Γ is the decay rate and $H(T_R)$ is the Hubble parameter at the decay epoch. Since the Hubble parameter is expressed as $H = \sqrt{g_*\pi^2/90}T_R^2/M_G$, where g_* is the number of mass-

less degrees of freedom ($= 43/4$) and M_G is the reduced Planck mass ($= 2.4 \times 10^{18}\text{GeV}$), the reheating temperature is estimated as $T_R = 0.554\sqrt{\Gamma M_G}$.

As mentioned above, the stringent constraint on the late-time entropy production or reheating temperature comes from the consideration of BBN. The long-lived massive particles which are responsible for the late-time entropy production should decay early enough to make the universe to be dominated by thermal radiation before the BBN epoch. To establish the thermal equilibrium, the decay products should be quickly thermalized through scatterings, annihilations, pair creations and further decays. Almost all standard particles except neutrinos are thermalized very soon when they are produced in the decay and subsequent thermalization processes. Neutrinos can be thermalized only through weak interaction which usually decouples at a few MeV. Thus, the thermalization of neutrinos is most important to obtain constraints on the reheating temperature. However, the thermalization of neutrinos has not been well studied and people have used various constraints on the reheating temperature between 1MeV and 10MeV. Therefore, in this letter, we will obtain the constraint on the reheating temperature by using the neutrino spectrum obtained from numerical integration of a set of Boltzmann equations together with full BBN network calculations.

Another interesting constraint may come from observations of anisotropies of the cosmic microwave background radiations (CMB). It is known that the CMB anisotropies are very sensitive to the time of matter-radiation equality (see e.g., [4]). When the reheating temperature is so low that sufficient neutrinos cannot be thermally produced, the radiation ($=$ photons + neutrinos) density becomes less than that in the standard case, which may give distinguishable signals in the CMB anisotropies. In this letter, we use the effective number of neutrino species N_ν^{eff} as a parameter which represents the energy density of neutrinos defined by $N_\nu^{\text{eff}} \equiv \sum_i \rho_{\nu_i} / \rho_{\text{std}}$, where $i = \nu_e, \nu_\mu, \nu_\tau$, and ρ_{std} is the neutrino energy density in

the standard case (i.e. no late-time entropy production).

First, let us discuss the neutrino spectrum. When a massive particle ϕ which is responsible for the late-time entropy production decays, all emitted particles except neutrinos are quickly thermalized and make a thermal plasma with temperature $\sim T_R$. If the reheating temperature is high enough ($T_R \gg 10$ MeV), there is no question about the neutrino thermalization. For relatively low reheating temperature ($T_R \lesssim 10$ MeV), however, neutrinos are slowly thermalized and may not be in time for the beginning of BBN. We assume that the decay branching ratio into neutrinos is very small and that neutrinos are produced only through annihilations of electrons and positrons, i.e. $e^+ + e^- \rightarrow \nu_i + \bar{\nu}_i$ ($i = e, \mu, \tau$). The evolution of the distribution function f_i of the neutrino ν_i is described by the Boltzmann equation:

$$\frac{\partial f_i(p_i, t)}{\partial t} - H p_i \frac{\partial f_i(p_i, t)}{\partial p_i} = C_i^a + C_i^s, \quad (1)$$

where p_i is the momentum of ν_i and C_i^a (C_i^s) is the collision term for annihilation (scattering) processes. Here we consider the following processes: $\nu_i + \nu_i \leftrightarrow e^+ + e^-$ and $\nu_i + e^\pm \leftrightarrow \nu_i + e^\pm$. We do not include the neutrino self interactions which may not change the result in the present paper, since the neutrino number densities are much smaller than the electron number density at low reheating temperature.

Here we have treated neutrinos as Majorana ones (i.e., $\nu = \bar{\nu}$). Note that our results are the same for Dirac neutrinos. The collision terms are quite complicated and expressed by nine dimensional integrations over momentum space. However, if we neglect electron mass and assume that electrons obey the Boltzmann distribution $e^{-p/T}$, the collision terms are simplified to one dimensional integration forms. Because the weak interaction rate is small at $T \lesssim 0.5$ MeV, neglecting the electron mass changes the result little. Then, C_i^a is given by [5]

$$C_i^a = - \int \frac{dp'_i}{\pi^2} p_i'^2 (\sigma v)_i (f_i(p_i) f_i(p'_i) - f_{eq}(p_i) f_{eq}(p'_i)), \quad (2)$$

where $f_{eq} = 1/(e^{p_i/T} + 1)$ is the equilibrium distribution and $(\sigma v)_i$ is the differential cross sections given by $(\sigma v)_e = (4G_F^2/(9\pi))((C_V + 1)^2 + (C_A + 1)^2)pp'$, and $(\sigma v)_{\mu, \tau} = (4G_F^2/(9\pi))(C_V^2 + C_A^2)pp'$. Here G_F is the Fermi coupling constant, and $C_A = -1/2, C_V = -1/2 + 2 \sin^2 \theta_W$ (θ_W : Weinberg angle).

As for scattering processes, C_i^s is expressed as

$$C_i^s = \frac{2G_F^2}{\pi^3} (C_V^2 + C_A^2) \times \left[-\frac{f_i}{p_i^2} \left(\int_0^{p_i} dp'_i (1 - f_i(p'_i)) F_1 + \int_{p_i}^\infty dp'_i (1 - f_i(p'_i)) F_2 \right) + \frac{1 - f_i(p_i)}{p_i^2} \left(\int_0^{p_i} dp'_i f_i(p'_i) B_1 + \int_{p_i}^\infty dp'_i f_i(p'_i) B_2 \right) \right]. \quad (3)$$

Here $(C_V^2 + C_A^2)$ is replaced by $((C_V + 1)^2 + (C_A + 1)^2)$ for $i = e$, and the functions F_1, F_2, B_1, B_2 are given by

$$\begin{aligned} F_1(p, p') &= D(p, p') + E(p, p') e^{-p'/T}, \\ F_2(p, p') &= D(p', p) e^{(p-p')/T} + E(p, p') e^{-p'/T}, \\ B_1(p, p') &= F_2(p', p), \quad B_2(p, p') = F_1(p', p), \end{aligned} \quad (4)$$

where

$$\begin{aligned} D(p, p') &= 2T^4(p^2 + p'^2 + 2T(p - p') + 4T^2), \\ E(p, p') &= -T^2[p^2 p'^2 + 2pp'(p + p')T \\ &\quad + 2(p + p')^2 T^2 + 4(p + p')T^3 + 8T^4]. \end{aligned} \quad (5)$$

Together with the above Boltzmann equations, we also solve the evolution of the densities of the massive particle ϕ , radiations $\rho_r (= \rho_\gamma + \rho_{e^\pm})$ and the scale factor a :

$$\frac{d\rho_\phi}{dt} = -\Gamma\rho_\phi - 3H\rho_\phi, \quad (6)$$

$$\frac{d\rho_r}{dt} = \Gamma\rho_\phi - \frac{d\rho_\nu}{dt} - 4H(\rho_r + \rho_\nu), \quad (7)$$

$$H = \frac{d \ln a}{dt} = \frac{1}{\sqrt{3}M_G} (\rho_\phi + \rho_r + \rho_\nu)^{1/2}, \quad (8)$$

where the neutrino density is given by $\rho_\nu = \sum_i 1/\pi^2 \int dp_i p_i p_i^3 f_i(p_i)$.

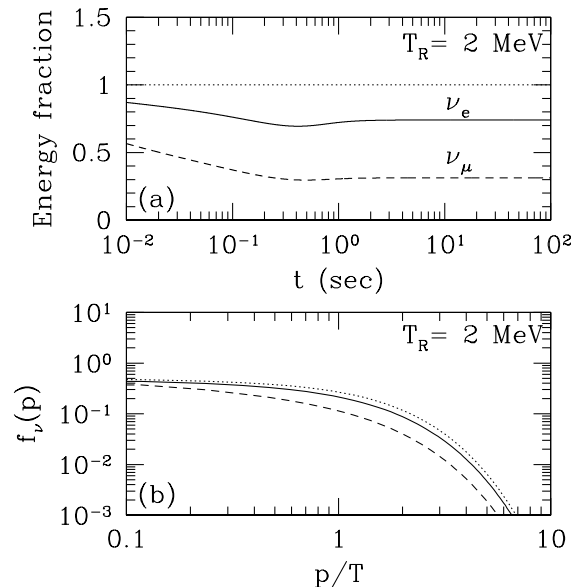


FIG. 1. (a) Evolution of the the energy density of ν_e (solid curve) and ν_μ (dashed curve) for $T_R = 2$ MeV. (b) Distribution of ν_e (solid curve) and ν_μ (dashed curve) for $T_R = 2$ MeV. The dotted curve is the thermal equilibrium Fermi-Dirac distribution.

In Fig. 1 (a) we show the evolutions of ρ_{ν_e} and $\rho_{\nu_\mu} = \rho_{\nu_\tau}$ for $T_R = 2$ MeV. Since the electron neutrinos interact with electrons or positrons through both charged and neutral currents, they are more effectively produced from

the thermal plasma than the other neutrinos which have only neutral current interactions. The final distribution functions f_e and $f_\mu = f_\tau$ are shown in Fig. 1 (b), from which one can see that the occupation numbers are close to equilibrium values at low momentum but they deviate significantly at higher momentum.

In Fig. 2 we can see the change of N_ν^{eff} as a function of T_R . If $T_R \gtrsim 7$ MeV, N_ν^{eff} is almost equal to three and neutrinos are thermalized very well. On the other hand, if $T_R \lesssim 7$ MeV, N_ν^{eff} becomes smaller than three.

The deficit of the neutrino distribution influences the produced light element abundances. In particular, the abundance of the primordial ${}^4\text{He}$ is drastically changed. At the beginning of BBN ($T \sim 1$ MeV - 0.1 MeV) the competition between the Hubble expansion rate and the weak interaction rates determines the freeze-out value of neutron to proton ratio. After the freeze-out time, neutrons can change into protons only through the free decay with the life time τ_n . Since the left neutrons are almost included into ${}^4\text{He}$, the primordial ${}^4\text{He}$ is sensitive to the freeze-out value of neutron to proton ratio.

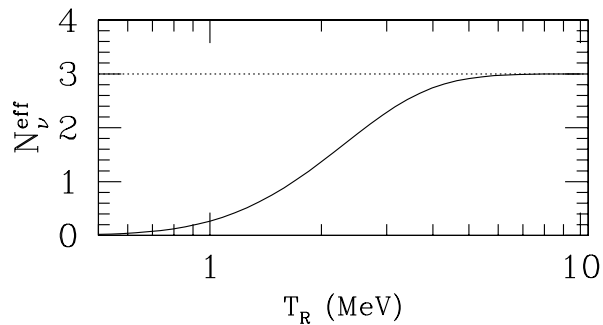


FIG. 2. N_ν^{eff} as a function of T_R .

If the neutrino energy density gets smaller than that of the standard BBN (SBBN), Hubble parameter is also decreased. Then the β equilibrium between neutrons and protons continues for longer time, and less neutrons are left. Thus, the predicted ${}^4\text{He}$ is less than the prediction of SBBN. This effect is approximately estimated by: $\Delta Y \simeq -0.1(-\Delta\rho/\rho)$, where Y is the mass fraction of ${}^4\text{He}$ and ρ is the total energy density of the universe.

In addition if the electron neutrino is not thermalized sufficiently and does not have the perfect Fermi-Dirac distribution, there are two interesting effects by which more ${}^4\text{He}$ are produced. The weak reaction rates are computed by the neutrino distributions which are obtained by solving Boltzmann equations. For example, a reaction rate at which neutron is changed into proton ($n + \nu_e \rightarrow p + e^-$) is represented by

$$\Gamma_{n\nu_e \rightarrow pe^-} = K \int_0^\infty dp_{\nu_e} \left[\sqrt{(Q + p_{\nu_e})^2 - m_e^2} (p_{\nu_e} + Q) p_{\nu_e}^2 \times \left(1 - \frac{1}{e^{(p_{\nu_e} + Q)/T_\gamma} + 1} \right) f_{\nu_e}(p_{\nu_e}) \right], \quad (9)$$

where $Q = m_n - m_p = 1.29$ MeV and K is a normalization factor which is determined by the neutron life time τ_n as $K \simeq (1.636\tau_n)^{-1}$. In this equation we can see that if the (anti) electron neutrino distribution functions decrease, the weak interaction rates also decrease.* First, when the weak interaction rate $\Gamma_{n \leftrightarrow p}$ decreases, the Hubble expansion becomes more rapid than that of the interaction rate earlier. Then the freeze-out value of neutron to proton ratio becomes larger than in SBBN and the predicted ${}^4\text{He}$ abundance becomes larger: $\Delta Y \simeq +0.15(-\Delta\Gamma_{n \leftrightarrow p}/\Gamma_{n \leftrightarrow p})$. Second when the interaction rates $\Gamma_{n \rightarrow p}$ at which neutrons are changed into protons become smaller, less neutrons can turn into protons after the freeze-out time. Then the produced ${}^4\text{He}$ also becomes larger: $\Delta Y \simeq +0.2(-\Delta\Gamma_{n \rightarrow p}/\Gamma_{n \rightarrow p})$.

As for the observational abundances, we adopt the following values. The primordial ${}^4\text{He}$ mass fraction Y is observed in the low metallicity extragalactic HII regions. Now we have two observational values, low ${}^4\text{He}$ and high ${}^4\text{He}$, which are reported by different groups. We take ‘‘Low ${}^4\text{He}$ ’’ from Olive, Skillman and Steigman (1997) [6], $Y^{\text{obs}} = 0.234 \pm (0.002)_{\text{stat}} \pm (0.005)_{\text{syst}}$. Recently Izotov et al. [7] claimed that the effect of the HeI stellar absorption which are not considered well in [6] is very important. We adopt their value as ‘‘High ${}^4\text{He}$ ’’, $Y^{\text{obs}} = 0.244 \pm (0.002)_{\text{stat}} \pm (0.005)_{\text{syst}}$.

The deuterium D/H is measured in the high redshift QSO absorption systems. Here we adopt the most reliable data $D/H = (3.39 \pm 0.25) \times 10^{-5}$ [8].

The ${}^7\text{Li}/\text{H}$ is observed in the Pop II old halo stars. We take the recent measurements [9] and adopt the additional larger systematic error, for fear there are underestimates in the stellar depletion and the production by the cosmic ray spallation. Then we obtain: $\text{Log}_{10}({}^7\text{Li}/\text{H}) = -9.76 \pm (0.012)_{\text{stat}} \pm (0.05)_{\text{syst}} \pm (0.3)_{\text{add}}$.

In order to discuss how the theoretical predictions with the late-time entropy production agree with the above observational constraints, we perform Monte Carlo calculation and the maximum likelihood analysis [for details, e.g. see [10]]. In Fig. 3 we plot the contours of the confidence level in the η - T_R plane for (a) Low ${}^4\text{He}$ and (b) High ${}^4\text{He}$. As we mentioned above, for $T_R \gtrsim 7$ MeV, the theoretical prediction is the same as SBBN. On the other hand as T_R decreases, Y gradually becomes smaller because the effective number of neutrino species N_ν^{eff} decreases. On the other hand, for $T_R \lesssim 2$ MeV the effect that the weak interaction rates are weakened due to the lack of the neutrino distributions begins to be important and Y begins to increase as T_R decreases. For $T_R \lesssim 1$

*The weak interaction rates with (anti) electron neutrino in the final state slightly increase because the Pauli blocking factor $(1-f_{\nu_e})$ increases. However, both of the total weak interaction rates $\Gamma_{n \rightarrow p}$ and $\Gamma_{p \rightarrow n}$ decrease.

MeV, the weak interaction rates are still more weakened and Y steeply increases as T_R decreases because it is too late to produce enough electrons and positrons whose mass is about $m_e = 0.511$ MeV. From Fig. 3 we can conclude that $T_R \lesssim 0.5$ MeV is excluded at 95 % C.L. Or we could rather say that T_R can be as low as 0.5 MeV. Accordingly N_ν^{eff} can be as small as 0.1.

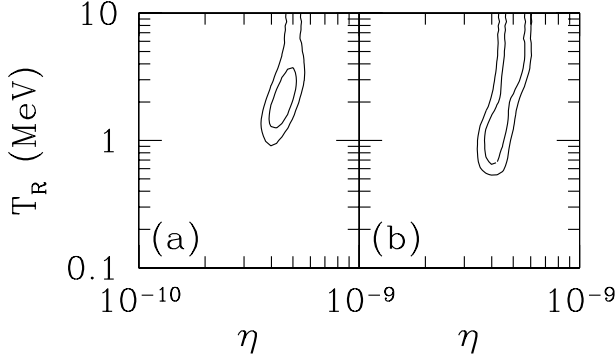


FIG. 3. Contours of the confidence levels in (η, T_R) plane for (a) observational value of Low ^4He and (b) High ^4He . The inner (outer) curve is 68% (95%) C.L..

The late time entropy production is also constrained from the formation of the large scale structure of the universe. We can fit the large scale galaxy distribution if the “shape parameter” $\Gamma_s \simeq 0.25 \pm 0.05$ [11]. In case of the standard cold dark matter (CDM) scenario, $\Gamma_s \equiv \Omega_0 h$ whose dependence is determined by the epoch of the matter-radiation equality. Here Ω_0 is the density parameter and h is the non-dimensional Hubble constant normalized by 100km/s/Mpc. Since $\Gamma_s \sim 0.5$ for so-called standard CDM model, it is known that this model is in serious trouble and one can achieve the desired fit with low density models where $\Omega_0 \simeq 0.3$. If the late time entropy production takes place, however, Γ_s is modified as $\Gamma_s = 1.68\Omega_0 h / (1 + 0.23N_\nu^{\text{eff}})$. Therefore the constraint from the large scale galaxy distribution becomes much tighter with $N_\nu^{\text{eff}} < 3$ (see Fig. 4).

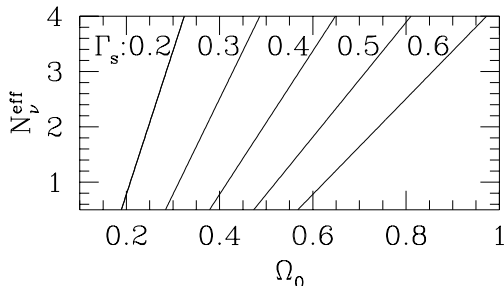


FIG. 4. Contours of $\Gamma_s = 0.2$ (bold), 0.3, 0.4, 0.5 and 0.6 on the $(\Omega_0, N_\nu^{\text{eff}})$ plane for $h = 0.7$.

Finally we discuss the CMB constraint on T_R . With the present angular resolutions and sensitivities of COBE observation [12] or current balloon and ground base ex-

periments, it is impossible to set a constraint on N_ν^{eff} . However it is expected that future satellite experiments such as MAP [13] and PLANCK [14] will give us a useful information about N_ν^{eff} . From Lopez et al.’s analysis [4], MAP and PLANCK have sensitivities that $\delta N_\nu^{\text{eff}} \gtrsim 0.1$ (MAP) and 0.03 (PLANCK) including polarization data, even if all cosmological parameters are determined simultaneously (see also Fig. 5). From such future observations of anisotropies of CMB, it is expected that we can precisely determine T_R .

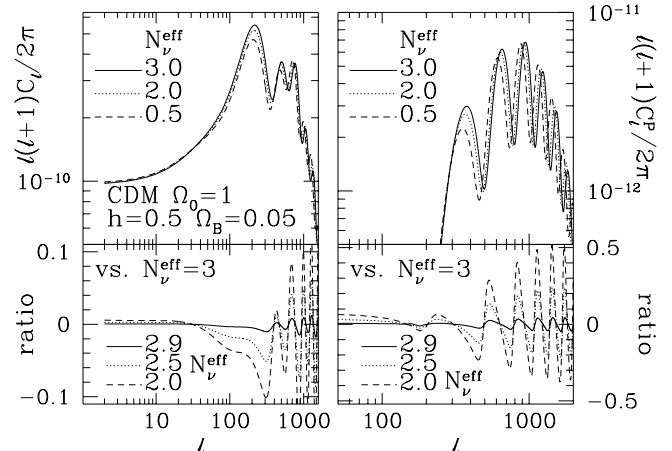


FIG. 5. Power spectra of CMB anisotropies (left top panel) and polarization (right top panel) of models with $N_{\text{eff}}^{\text{eff}} = 3, 2$ and 0.5. Bottom two panels show $(C_\ell(N_{\text{eff}}) - C_\ell(3))/C_\ell(3)$ with $N_{\text{eff}}^{\text{eff}} = 2.9, 2.5$ and 2 for CMB anisotropies (left bottom) and polarization (right bottom).

-
- [1] E.W. Kolb and M.S. Turner, *The Early Universe* (Addison-Wesley, 1989).
 - [2] For a review, H.P. Nilles, *Phys. Rep.* **110** (1984) 1.
 - [3] C.D. Coughlan et al., *Phys. Lett.* **B131** (1983) 59.
 - [4] R.E. Lopez, S. Dodelson, A. Heckler and M.S. Turner, astro-ph/9803095.
 - [5] M. Kawasaki, G. Steigman and H-S Kang, *Nucl. Phys.* **B403** (1993) 671; M. Kawasaki et al., *Nucl. Phys.* **B419** (1994) 105; M. Kawasaki, K. Kohri and K. Sato, *Phys. Lett.* **B430** (1998) 671.
 - [6] K.A. Olive, G. Steigman, and E.D. Skillman, *Astrophys. J.* **483** (1997) 788.
 - [7] Y.I. Izotov, T.X. Thuan, and V.A. Lipovetsky, *Astrophys. J. Suppl. Series*, **108** (1997) 1; Y.I. Izotov and T.X. Thuan *Astrophys. J.*, **500** (1998) 188.
 - [8] S. Burles and D. Tytler, *Astrophys. J.* **507** (1998) 732.
 - [9] P. Bonifacio and P. Molaro, *Mon. Not. Roy. Astron. Soc.* **285** (1997) 847.
 - [10] E. Holtmann, M. Kawasaki, K. Kohri and T. Moroi, To appear in *Phys. Rev.* **D**, hep-ph/9805405.
 - [11] J.A. Peacock and S.J. Dodds, *Mon. Not. Roy. Astron. Soc.* **267**, 1020 (1994).
 - [12] C.L. Bennett et al., *Astrophys. J. Letter* **464**, L1 (1996).
 - [13] <http://map.gsfc.nasa.gov/>
 - [14] <http://astro.estec.esa.nl/SA-general/Projects/Planck/>